

# Infrared spectroscopy of ZnO nanoparticles containing CO<sub>2</sub> impurities

W. M. Hlaing Oo and M. D. McCluskey<sup>a)</sup>

Department of Physics, Washington State University, Pullman, Washington 99164-2814

A. D. Lalonde and M. G. Norton

School of Mechanical and Materials Engineering, Washington State University, Pullman, Washington 99164-2920

(Received 8 November 2004; accepted 21 December 2004; published online 9 February 2005)

Impurities play a major role in determining the optical and electrical properties of semiconductor nanoparticles. In this work, the presence and source of CO<sub>2</sub> impurities in ZnO nanoparticles were studied by IR absorption spectroscopy. Isotopic substitution was used to verify the vibrational frequency assignment. Isochronal annealing experiments were performed to study the formation and stability of the molecular impurities. Our results indicate that the molecules are much more stable than CO<sub>2</sub> adsorbed on bulk ZnO surfaces. By comparing our observations with similar results from IR spectroscopy of CO<sub>2</sub> trapped in carbon nanotubes [C. Matranga, L. Chen, M. Smith, E. Bittner, J. K. Johnson, and B. Bockrath, *J. Phys. Chem. B* **107**, 12930 (2003)], we conclude that the molecules are trapped in the ZnO nanoparticles. © 2005 American Institute of Physics. [DOI: 10.1063/1.1866511]

Zinc oxide (ZnO) is a wide-band gap semiconductor that is desirable for many applications, such as piezoelectric transducers, varistors, gas sensors, and transparent conducting thin films.<sup>1-5</sup> By reducing the size of ZnO crystals to nanoscale dimensions, researchers can tailor the properties via quantum confinement and surface effects. ZnO nanoparticles have been synthesized by a variety of wet-chemistry methods. The use of precursor materials such as zinc acetate, zinc nitrate, or zinc carbonate provides an efficient way to synthesize the ZnO particles.<sup>6-8</sup> However, a major potential problem is the presence of impurities remaining from the precursor materials and reaction products. These contaminants can dramatically affect the electrical and optical properties of the nanoparticles. Recently, Orlinskii *et al.*<sup>9</sup> reported that Li and Na impurities act as shallow donors in ZnO nanoparticles. The hydroxyl (OH) group on the surface plays an important role in the luminescence properties of ZnO quantum dots.<sup>7</sup> In this letter, we report the presence of CO<sub>2</sub> molecules in ZnO nanoparticles, observed by IR spectroscopy. Our results reveal that the CO<sub>2</sub> impurities are formed by reactions involving the organic precursors.

The synthesis method described in Ref. 10 was used in this work. Zinc acetate dihydrate [Zn(CH<sub>3</sub>COO)<sub>2</sub>·2H<sub>2</sub>O] and sodium hydrogen carbonate (NaHCO<sub>3</sub>) were mixed thoroughly at room temperature, with a molar ratio of 1:2.4. The mixture was sealed in an evacuated quartz ampoule filled with 2/3 atm argon gas. In this way, we could prevent contamination from ambient air during the reaction. The reaction was performed at 200 °C for 3 h. After the reaction process, the product was washed several times with distilled water to remove the by-product sodium acetate (CH<sub>3</sub>COONa), and dried at room temperature overnight. The powder was pressed into a thin pellet (thickness ~0.25 mm) and then annealed in argon at 350 °C for 2 h to remove the remaining water. A transmission electron microscope (TEM) image of the ZnO particles is shown in Fig. 1. The particles were roughly spherical, with a size of about 20 nm. The crystal

structure was examined by powder X-ray diffraction (XRD) analysis. Three dominant peaks in the XRD spectrum confirmed the hexagonal wurtzite structure (Fig. 2), in agreement with previous work.<sup>10</sup>

Room temperature IR absorption spectra were obtained with a Bomem DA8 vacuum Fourier-transform infrared spectrometer with a liquid nitrogen cooled HgCdTe detector. The instrumental resolution was 4 cm<sup>-1</sup>, and the spectra were averaged over 500 scans. As shown in Fig. 3(a), a strong IR absorption peak was observed at a frequency of 2342 cm<sup>-1</sup>. In addition, a weak absorption peak was observed at 2277 cm<sup>-1</sup>. These peaks are assigned to asymmetric stretch frequencies ( $\nu_3$ ) of <sup>12</sup>CO<sub>2</sub> and <sup>13</sup>CO<sub>2</sub> molecules, respectively. For a linear free CO<sub>2</sub> molecule, the  $\nu_3$  vibrational frequency is estimated by

$$\nu = \sqrt{\kappa \left( \frac{2}{M_C} + \frac{1}{M_O} \right)}, \quad (1)$$

where  $M_C$  and  $M_O$  are the masses of carbon and oxygen respectively, and  $\kappa$  is an effective spring constant. The cal-

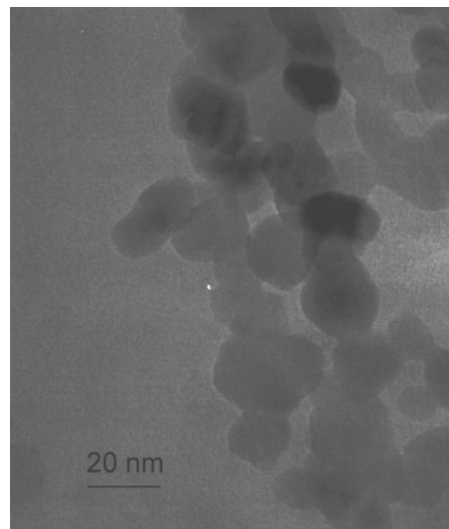


FIG. 1. TEM image of ZnO nanoparticles.

<sup>a)</sup>Electronic mail: mattmcc@wsu.edu

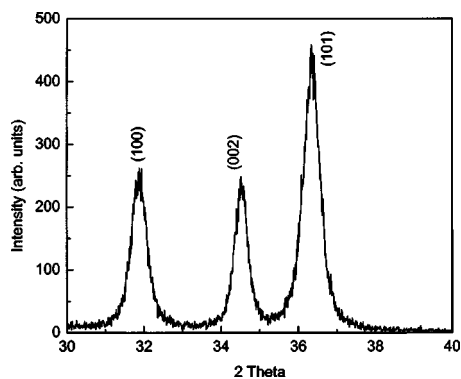
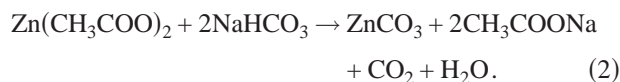


FIG. 2. XRD spectrum of ZnO nanoparticles.

culated frequency ratio  $\nu(^{12}\text{CO}_2)/\nu(^{13}\text{CO}_2)$  is 1.029, in good agreement with the observed ratio of 1.028. The ratio of peak intensities is in agreement with the natural isotopic abundance ( $[^{13}\text{C}]/[^{12}\text{C}]=0.01$ ). Broad absorption peaks in the region between  $1200$  and  $1700\text{ cm}^{-1}$ , not shown here, were also observed. Those absorption bands are due to vibrations of carbonates ( $\text{ZnCO}_3$ ).<sup>11</sup>

To obtain more conclusive results, the same synthesis procedure was repeated with isotopically enriched precursor materials. Zinc acetate crystals with different  $^{13}\text{C}$  compositions were produced by reaction of dilute acetic acid ( $\text{CH}_3\text{COOH}$ ) and pure ZnO powder. The details of the precursor materials for each sample are given in Table I. IR absorption peaks for each ZnO sample prepared from different precursors are shown in Fig. 3. The results indicate that the peak at  $2277\text{ cm}^{-1}$  increases with increasing  $^{13}\text{C}$  composition in the precursors. Hence, we conclude that the  $\text{CO}_2$  molecules originate from the organic precursors.

The formation of  $\text{CO}_2$  can be explained by a two-step reaction. First, zinc acetate reacts with sodium hydrogen carbonate, producing zinc carbonate and sodium acetate



The product, zinc carbonate, then decomposes into ZnO and  $\text{CO}_2$  by thermal decomposition

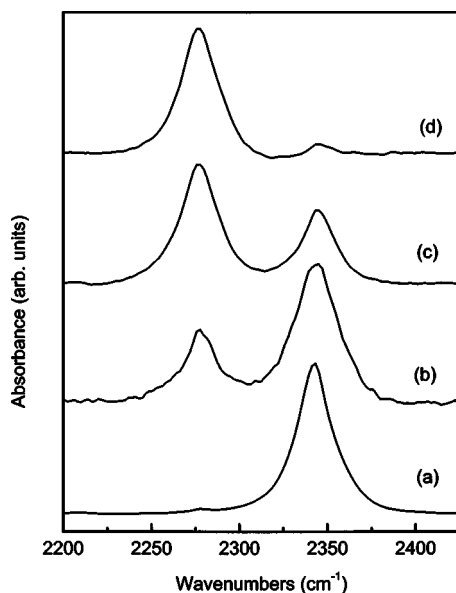
FIG. 3. IR Absorption spectra of ZnO nanoparticles with different  $^{13}\text{C}$  compositions (see Table I).

TABLE I. Isotopic compositions of precursor materials used to synthesize ZnO nanoparticle samples.

Samples	Precursor materials
(a)	$\text{Zn}(\text{CH}_3\text{COO})_2$ and $\text{NaHCO}_3$ (natural isotopic abundance)
(b)	$\text{Zn}(\text{CH}_3\text{COO})_2$ and $\text{NaH}^{13}\text{CO}_3$
(c)	$\text{Zn}(\text{CH}_3^{13}\text{COO})_2$ and $\text{NaH}^{13}\text{CO}_3$
(d)	$\text{Zn}(^{13}\text{CH}_3^{13}\text{COO})_2$ and $\text{NaH}^{13}\text{CO}_3$

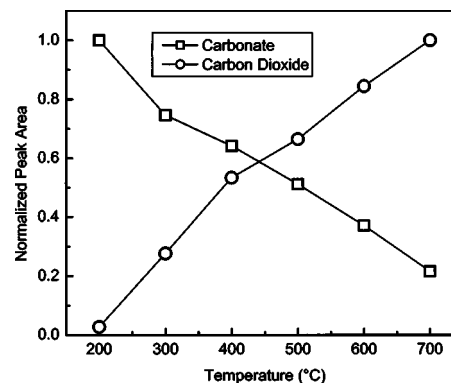


These reactions account for the observed IR absorption peaks of carbonates, which remain in the samples. Since zinc carbonate is insoluble in water, one cannot simply remove unreacted zinc carbonate by washing with water. The zinc carbonate therefore remains in the sample and acts as a source of  $\text{CO}_2$ .

To further investigate the formation and stability of  $\text{CO}_2$  in nanoparticles, isochronal annealing experiments were performed. The annealing process was carried out in an open-air furnace, over a temperature range of  $200$ – $700\text{ }^\circ\text{C}$ . Samples (with natural isotopic abundance) were annealed for a duration of 1 h at each temperature. IR spectra were taken after each annealing step. As shown in Fig. 4, the intensity of the  $\text{CO}_2$  vibrational peak increases with increasing temperature. Correspondingly, the carbonate peaks decrease upon annealing. These observations are in agreement with our model assumption that zinc carbonate is a source of  $\text{CO}_2$  impurities.

Finally, the possibility of  $^{12}\text{CO}_2$  contamination from ambient air was investigated. Figure 5 shows IR spectra of samples, with the same  $^{13}\text{C}$  composition as sample (d), prepared in air and argon ambients. Despite the absence of  $^{12}\text{C}$  atoms in the precursors, a strong absorption peak at  $2342\text{ cm}^{-1}$  appeared for the sample prepared in air. This effect is presumably due to isotope exchange of  $^{13}\text{C}$  and  $^{12}\text{C}$  during the reaction at  $200\text{ }^\circ\text{C}$ . Postgrowth annealing of sample (d) in  $^{12}\text{CO}_2$  gas did not result in an increase in the  $^{12}\text{CO}_2$  peak, indicating that isotope exchange occurs only during the first reaction [Eq. (2)]. During postgrowth annealing, therefore,  $\text{CO}_2$  molecules are produced only by thermal decomposition of the remaining carbonates in the sample and not from the ambient.

To understand the nature of  $\text{CO}_2$  bonding to ZnO, we compared our results with those of  $\text{CO}_2$  adsorption studies on ZnO surfaces.<sup>11,12</sup> In the adsorption process,  $\text{CO}_2$  reacts with ZnO and forms chemical species such as bidentate car-

FIG. 4.  $\text{CO}_2$  and carbonate peak intensities in ZnO nanoparticles after isochronal annealing. Peaks are normalized to their maxima.

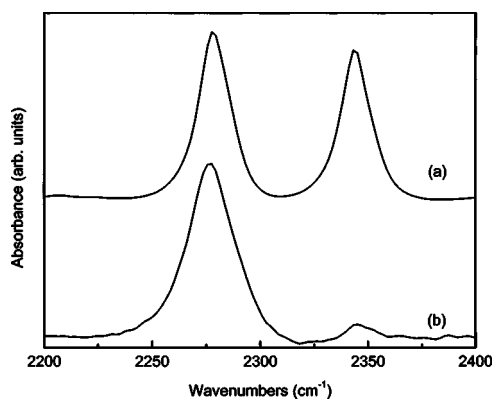


FIG. 5. IR absorption spectra of ZnO nanoparticles, (a) prepared in air, (b) prepared in argon gas. The precursors contained only  $^{13}\text{C}$  isotopes [sample (d)].

bonates, polydentate carbonates, and linear  $\text{CO}_2$ .<sup>12</sup> The linear molecules, which have vibrational frequencies similar to those of free  $\text{CO}_2$ , are weakly adsorbed and are not stable. They can be immediately removed by evacuation at room temperature. This observation is different from our results, since  $\text{CO}_2$  impurities in our samples are stable even at elevated temperatures.

Interestingly, our results are similar to studies of trapped  $\text{CO}_2$  molecules in carbon nanotube bundles, recently reported by Matranga *et al.*<sup>13</sup> In their work, IR spectroscopy showed that thermal decomposition of oxygen-containing functionalities on carbon nanotubes generated  $\text{CO}_2$  molecules that became permanently trapped in the nanotube bundles. The absorption band of trapped  $\text{CO}_2$  was centered at  $2330\text{ cm}^{-1}$ , which is close to that of the free molecule. They observed that those trapped molecules persist after multiple temperature cycles and are stable for as long as two months in a vacuum chamber. These results are qualitatively similar to ours. In the present work, however, it is not known exactly

where the  $\text{CO}_2$  molecules reside. It is possible, for example, that  $\text{CO}_2$  molecules become trapped inside voids in ZnO nanoparticles.

In conclusion, we have observed the presence of  $\text{CO}_2$  impurities in ZnO nanoparticles by IR spectroscopy. Isotopic substitution was used to confirm the vibrational frequency assignment. The  $\text{CO}_2$  is formed by thermal decomposition of zinc carbonate, which is a reaction product. The molecules are believed to be trapped within the particles, but their exact location is not known. Further studies on the role of  $\text{CO}_2$  impurities on the electrical and optical properties of ZnO nanoparticles will be of considerable practical interest.

The authors are pleased to acknowledge A. Punnoose for providing samples for preliminary experiments. This work was supported in part by the National Science Foundation under Grant No. DMR-0203832. Acknowledgement is made to the Donors of the American Chemical Society Petroleum Research Fund for partial support of this research.

<sup>1</sup>Z. L. Wang, *J. Phys.: Condens. Matter* **16**, R829 (2004).

<sup>2</sup>D. C. Look, *Mater. Sci. Eng., B* **80**, 383 (2001).

<sup>3</sup>S. J. Pearton, D. P. Norton, K. Ip, Y. W. Yeo Heo, and T. Steiner, *J. Vac. Sci. Technol. B* **22**, 932 (2004).

<sup>4</sup>T. Minami, *MRS Bull.* **25**, 38 (2000).

<sup>5</sup>J. F. Wager, *Science* **300**, 1245 (2003).

<sup>6</sup>L. Spanhel and M. A. Anderson, *J. Am. Chem. Soc.* **113**, 2826 (1991).

<sup>7</sup>H. Zhou, H. Alves, D. M. Hofmann, B. K. Meyer, G. Kaczmarczyk, A. Hoffmann, and C. Thomsen, *Phys. Status Solidi B* **229**, 825 (2002).

<sup>8</sup>T. Katsuyama and A. Kimura, U. S. Patent No. 6,1715,80 (9 Jan 2001).

<sup>9</sup>S. B. Orlinskii, J. Schmidt, P. G. Baranov, D. M. Hofmann, C. M. Donega, and A. Meijerink, *Phys. Rev. Lett.* **92**, 047603 (2004).

<sup>10</sup>Z. Wang, H. Zhang, L. Zhang, J. Yuan, S. Yan, and C. Wang, *Nanotechnology* **14**, 11 (2003).

<sup>11</sup>J. H. Taylor and C. H. Amberg, *Can. J. Chem.* **39**, 535 (1961).

<sup>12</sup>J. Saussey, J. C. Lavalley, and C. Bovet, *J. Chem. Soc., Faraday Trans. 1* **78**, 1457 (1982).

<sup>13</sup>C. Matranga, L. Chen, M. Smith, E. Bittner, J. K. Johnson, and B. Bockrath, *J. Phys. Chem. B* **107**, 12930 (2003).